

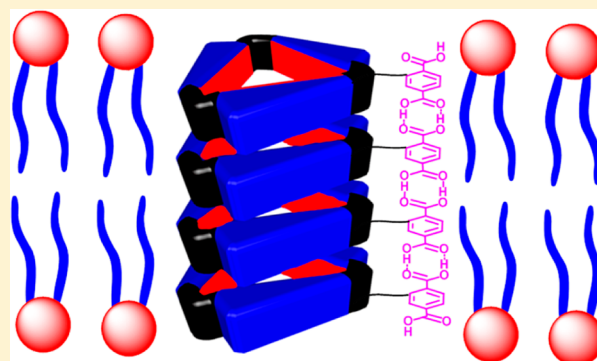
Tuning Nanopore Formation of Oligocholate Macrocycles by Carboxylic Acid Dimerization in Lipid Membranes

Lakmini Widanapathirana and Yan Zhao*

Department of Chemistry, Iowa State University, Ames, Iowa 50011-3111, United States

S Supporting Information

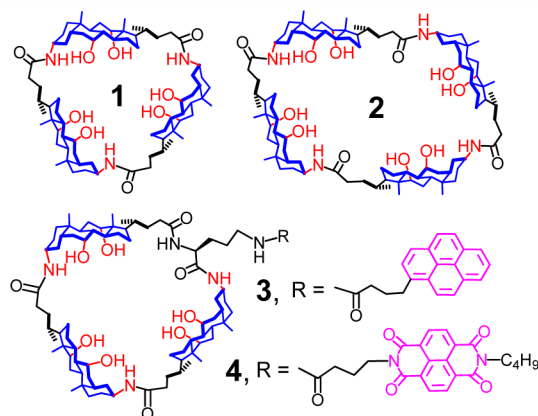
ABSTRACT: Oligocholate macrocycles self-assemble into transmembrane nanopores by the associative interactions of water molecules inside the amphiphilic macrocycles. Macrocycles functionalized with a terephthalic acid “side chain” displayed significantly higher transport activity for glucose across lipid bilayers than the corresponding methyl ester derivative. Changing the 1,4-substitution of the dicarboxylic acid to 1,3-substitution lowered the activity. Combining the hydrophobic interactions and the hydrogen-bond-based carboxylic acid dimerization was an effective strategy to tune the structure and activity of self-assembled nanopores in lipid membranes.



Lipid membranes are the barriers that separate the inside of a cell from its environment and the various compartments within the cell from the cytosol. Numerous biological functions occur at these interfaces,¹ and not surprisingly, membrane proteins account for nearly 50% of all drug targets.² For these reasons, understanding how molecules recognize one another in a lipid membrane is of great importance to both biology and chemistry. In the past decades, chemists have gained significant understanding of how molecular recognition occurs in solution. However, when molecules move from a homogeneous solution into an amphiphilic, nanodimensioned, and liquid crystalline membrane, their intermolecular interactions (including those with the environment) change enormously and the relative importance of different noncovalent forces often needs recalibration.

Our group has reported amphiphilic (oligocholate) foldamers prepared from cholic acid.³ Their steroid-derived backbone and controlled conformations make them excellent mimics of membrane protein transporters.⁴ More recently, we prepared oligocholate macrocycles (e.g., 1–2) as novel pore-forming agents.⁵ The numerous inward-facing hydroxyl and amide groups make the molecule carry a pool of water in the interior when it enters a membrane. Because these water molecules have a strong tendency to interact with other water molecules instead of the lipid hydrocarbon, the macrocycles prefer to stack over one another to form a transmembrane nanopore. The pore formation was confirmed by the macrocycle-induced leakage of glucose from liposomes⁵ and further by fluorescently (e.g., 3–4) and isotopically labeled analogues using fluorescence⁶ and solid-state NMR spectroscopy, respectively.⁷

Nanopore-forming agents have numerous applications in drug delivery, separation, sensing, and catalysis.⁸ For many of

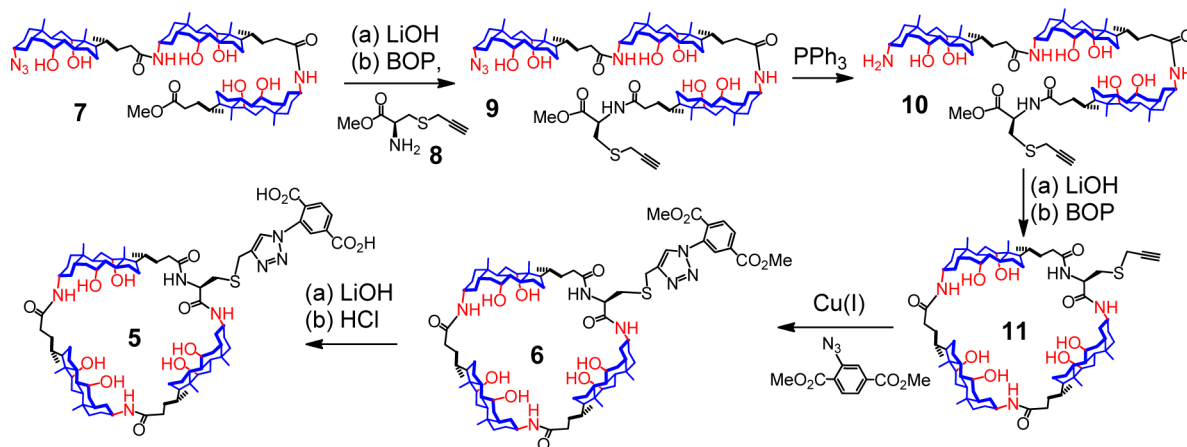


these applications, it is highly desirable that the pore formation be controlled rationally. Compound 5 contains a tricholate macrocycle and a terephthalic acid side chain. Terephthalic acid is known to have two crystalline forms and, in both forms, the molecules are linked together by hydrogen-bonded carboxylic acid dimers into infinite chains.⁹ Our idea was that a combination of the hydrophobic interactions (among the entrapped water molecules inside the cholate macrocycles) and a tunable, directional polar interactions (among the carboxylic acids on the side chain) would allow us to control the pore formation.¹⁰ Since the height of the cholate macrocycle is similar to the width of a cyclohexane, the hydrogen-bonding interactions of the terephthalic acid and the stacking of the cholate macrocycle should be compatible geometrically.

Received: March 5, 2013

Published: April 11, 2013

Scheme 1. Synthesis of Terephthalic Acid Functionalized Macrocycle 5



Compound **5** was obtained by the hydrolysis of ester **6**, which was synthesized from the linear tricholate **7** by standard transformations (Scheme 1). The key design of the molecule involves the incorporation of a natural L-cysteine functionalized with a propargyl group. The terminal alkyne allowed a late-stage installation of the terephthalic acid moiety via a convenient click reaction. It also enables us to change the carboxylic side chain of the macrocycle readily (*vide infra*).

The tricholate macrocycle has a triangularly shaped internal cavity approximately 1 nm on the side, large enough for glucose to pass through.⁵ Figure 1 compares the leakage profiles of

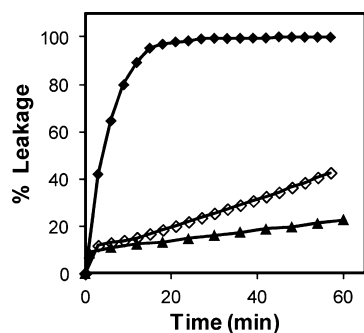


Figure 1. Percent leakage of glucose from POPC/POPG LUVs as a function of time for macrocycle **5** (◆), macrocycle **6** (◇), and linear trimer **7** (▲). [Oligocholate] = 5.0 μM . [Phospholipids] = 104 μM .

glucose-filled large unilamellar vesicles (LUVs) induced by the terephthalic acid-functionalized macrocycle (**5**), its methyl ester derivative (**6**), and the linear trimer (**7**). The leakage assay was based on the reactions between the escaped glucose and extravesicular enzymes that released UV-active NADPH.¹¹ Whereas the linear trimer showed little activity over the background leakage (averaging 6–10% at 60 min), the macrocycles displayed higher activity. The acid derivative was by far the most effective transporter among the three, with all 300 mM of glucose leaking out of the liposomes in <20 min in the presence of 5 μM of **5**.

Most membrane transporters function as either a carrier or a channel/pore.¹² A carrier binds and accompanies its cargo to diffuse across the membrane. A channel or pore, on the other hand, is relatively stationary within the membrane. One way to distinguish pore-based transport from a carrier-based mechanism is to study the effect of lipid composition on the transport

rate. Addition of 30% cholesterol to the POPC/POPG membrane is known to increase the hydrophobic thickness of the membrane from 2.6 to 3.0 nm¹³ and decrease its fluidity.¹⁴ Although cholesterol reduces the membrane permeability of hydrophilic molecules in general,¹⁵ cholesterol incorporation was found to *speed up* the glucose transport by macrocycles **1** and **2** across POPC/POPG membranes.⁵ The result was counterintuitive according to conventional reasoning but fully consistent with the hydrophobically driven pore formation.

To our surprise, the addition of 30 mol % of cholesterol to the POPC/POPG membranes did not enhance significantly the glucose leakage induced by **5** (Figure 2a). Although the leakage

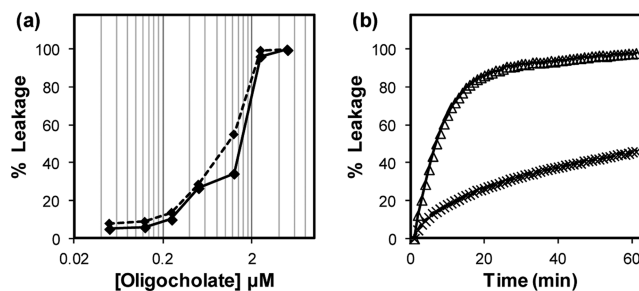


Figure 2. (a) Percent leakage of glucose at 30 min induced by **5** from POPC/POPG LUVs with (dashed line) and without 30% cholesterol (solid line). [Phospholipids] = 104 μM . (b) Percent leakage of CF induced by **5** from POPC/POPG LUVs with (x) and without 30% cholesterol (Δ). [Oligocholate] = 0.5 μM . [Phospholipids] = 2.9 μM . The leakage experiments were typically run in duplicate.

overall was still slightly higher for the cholesterol-containing liposomes, the effect was far smaller than that observed for **1** and **2** (up to 5–7 times faster with the same level of cholesterol, depending on the concentration of the macrocycle).⁵

Figure 1 shows that the carboxylic acids were clearly beneficial to the glucose transport across the POPC/POPG membranes. Could it be possible that other mechanisms (than nanopore formation) was responsible for the faster leakage of **5** over **6**? To better understand the transport mechanism, we switched the permeant to carboxyfluorescein (CF), a molecule too large to permeate the cyclic tricholate nanopore. CF displays strong self-quenching above 50 mM and, thus, emits more strongly once escaping from a liposome.¹⁶ Our previous study suggests that CF needs to be sandwiched by two cyclic

tricholates to move across a membrane via a carrier mechanism.¹⁷ As shown in Figure 2b, the CF leakage induced by **5** slowed down greatly upon the inclusion of cholesterol in the LUVs. At 60 min, the cholesterol-containing liposomes (×) only showed less than half of the leakage found in the cholesterol-free ones (△).

The above experiments demonstrated that cholesterol was indeed detrimental to carrier-based transport, in agreement with other literature work.¹⁸ The study also assured us that, despite the small enhancement in the glucose leakage caused by cholesterol incorporation, macrocycle **5** did NOT function as a carrier for glucose. If we “normalize” the cholesterol effect on the glucose transport over its (negative) impact on the CF transport, we could still conclude that the glucose leakage induced by **5** from the cholesterol-containing liposomes in Figure 2a was unusually high.

After ruling out the carrier mechanism, we performed the lipid-mixing assay to verify the integrity of the lipid bilayers. In the lipid-mixing assay, a batch of unlabeled LUVs is mixed with another batch labeled with 1 mol % of NBD- and rhodamine-functionalized lipids. If the carboxylic acid-functionalized **5** destabilized the liposomes by other mechanisms (e.g., membrane fusion or destruction), the fluorescence resonance energy transfer (FRET) between the fluorescent labels would be affected.¹⁹ In our hands, even at the highest concentration studied (5 mol %), the liposomes showed <16% mixing (Figure 3a), indicating that none of the above-mentioned membrane-

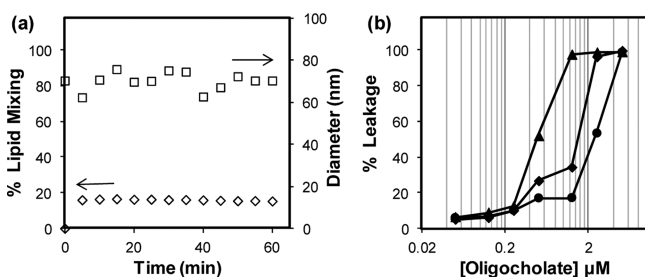


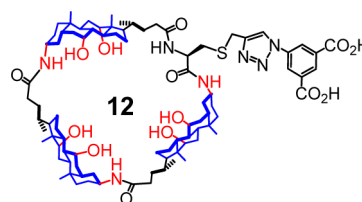
Figure 3. (a) Percent lipid-mixing and the size of the POPC/POPG LUVs upon the addition of **5**. [**5**] = 2.5 μM, [phospholipids] = 54.0 μM. (b) Percent leakage of glucose at 30 min induced by **1** (▲), **5** (◆), and **12** (●) from POPC/POPG LUVs. [Phospholipids] = 104 μM.

disrupting processes was significant in the presence of **5**. The conclusion was also supported by dynamic light scattering (DLS) showing nearly constant size of the liposomes after the addition of **5** (Figure 3a).

At this point, it seems reasonable to conclude that (a) the carboxylic acids in macrocycle **5** were beneficial to the glucose transport across the membrane and (b) the transport bore essentially all the important hallmarks of the hydrophobically driven pore-forming mechanism. The only “abnormality” was the smaller enhancement of glucose transport upon cholesterol inclusion in the membrane. The observation, however, is not difficult to understand from the viewpoint of polarity. Cholesterol increases the hydrophobicity of the membrane.¹³ Although the stronger environmental hydrophobicity facilitates the stacking of cholate macrocycles,⁵ it probably lowers the solubility of polar compounds including the terephthalic acid-containing **5**. Even if the carboxylic acid dimer may be stronger in the more hydrophobic, cholesterol-containing membrane, the overall lower concentration of **5** within the membrane

would represent a counterbalancing effect for the pore formation. This could also be one reason why **5** was still less effective in the glucose transport than the parent macrocycle **1** (Figure 3b).²⁰

If indeed the carboxylic acid dimerization from the terephthalic acid side chains and the hydrophobically driven stacking of the cholate macrocycles were collectively responsible for the high activity of **5**, altering the dicarboxylic acids should allow one to tune the transport activity. We thus prepared a corresponding “carboxylic acid isomer”, i.e., **12**, following a similar click coupling. Unlike terephthalic acid that forms a chain-like structure commensurate with the stacked nanopore, 5-substituted isophthalic acid derivatives tend to adopt cyclic hexameric structures through the carboxylic acid dimerization.²¹ Since the stacked cholate macrocycles prefer a linear alignment of the functionalized side chains, isophthalic acid should be less than ideal.



The above postulation was confirmed in our glucose leakage assay. The isophthalic acid-functionalized macrocycle consistently underperformed its *para* isomer as a glucose transporter (Figure 3b), indicating that the orientation of the carboxylic acids was critical to the transport. The result further ruled out “generic” effects of carboxylic acids on the membrane. If compound **5**, for example, simply causes glucose leakage by its amphiphilicity, with the terephthalic acid acting as a hydrophilic moiety, it is difficult to imagine that switching the 1,4-substitution to 1,3 would have a large effect on the transport, especially when there are numerous rotatable bonds between the acid-containing phenyl group and the cholate macrocycle.

The importance of carboxylic acid dimerization in membrane is also supported by the literature. When bound to lipid membranes, fatty acids shift their pK_a from ca. 4 in solution to 7.5.²² In the protonated, uncharged form, a fatty acid can migrate into a lipid membrane and rapidly diffuse to the other side. The half-life of the flip-flop of fatty acids in common lipid bilayers is <10 ms.²³ Thus, these acids have no difficulty traversing the membrane, most likely because their dimerization lowers the polarity of the carboxylic acids and make them compatible with nonpolar environments.

In summary, carboxylic acid dimerization could be used to rationally tune the hydrophobically driven pore formation of cholate macrocycles. Our previous experience tells us that molecular recognition in membrane could differ enormously from that in solution. The aromatic donor–acceptor interactions between 1,5-dialkoxynaphthalene and NDI, for example, were found to be 1–2 orders of magnitude stronger than the acceptor–acceptor interactions in polar solvents.²⁴ For the cholate macrocycles, however, **4** transported glucose more efficiently than either **3** or the 1:1 3/4 mixture.²⁵ The result suggested the acceptor–acceptor interactions were more effective at promoting the stacking of the cholate macrocycles in lipid membranes. Another work of ours indicates that the strong guanidinium–carboxylate salt bridge was rather ineffective at promoting stacking of the cholate macrocycles, due to the strong preference of these polar groups for

membrane surface.¹⁰ This work shows that carboxylic acid side chains can be used to regulate the stacking of cholate macrocycles effectively. As chemists become interested in creating functional structures in lipid membranes, the carboxylic acid dimer²⁶ may be a particularly useful motif for supramolecular construction.²⁷

EXPERIMENTAL SECTION

The preparation of LUVs, the procedures for the leakage assays, and the lipid mixing assay were reported previously.⁵ Compound 7,²⁸ compound 8,²⁹ methyl 2-azidoterephthalate,³⁰ and 5-azidoisophthalic acid³⁰ were synthesized according to literature procedures.

Compound 9. The carboxylic acid of 7²⁸ (450 mg, 0.37 mmol), 8 (83 mg, 0.48 mmol), 1-hydroxybenzotriazole (HOBt, 89 mg, 0.66 mmol), and (benzotriazol-1-yloxy)tris(dimethylamino)phosphonium hexafluorophosphate (BOP, 292 mg, 0.66 mmol) were dissolved in anhydrous DMF (2 mL). *N,N*-Diisopropylethylamine (DIPEA, 0.51 mL, 2.93 mmol) was added. The mixture was allowed to react in a microwave reactor at 100 °C for 1 h and monitored by TLC. When the reaction was complete, the mixture was cooled to room temperature and poured into a dilute HCl solution (0.05 M, 250 mL). The precipitate was collected, dried, and purified by column chromatography over silica gel, using 12:1 CH₂Cl₂/CH₃OH as the eluent to give a light brown powder (272 mg, 55%). ¹H NMR (400 MHz, CDCl₃/CD₃OD = 1:1, δ): 4.70 (br, 1H), 3.93 (br, 3H), 3.79 (br, 3H), 3.73 (s, 3H), 3.50 (br, 2H), 3.25 (s, 1H), 3.17 (m, 2H), 2.95 (m, 1H), 2.93 (m, 1H), 2.43 (t, 1H), 2.38–1.0 (a series of m), 0.66 (s, 9H). ¹³C NMR (100 MHz, CDCl₃/CD₃OD = 1:1, δ): 176.0, 174.8, 172.2, 79.7, 73.3, 72.4, 68.5, 62.0, 52.7, 52.3, 47.6, 46.7, 42.4, 39.9, 36.5, 36.2, 35.2, 34.0, 33.4, 32.4, 28.8, 27.1, 23.6, 23.0, 19.7, 17.6, 12.9. ESI MS (*m/z*): [M + Na]⁺ calcd for C₇₉H₁₂₆N₆NaO₁₁S 1389.9098, found 1390.9079.

Compound 10. A solution of compound 9 (155 mg, 0.110 mmol) and triphenylphosphine (60 mg, 0.230 mmol) in methanol (4 mL) was heated to reflux overnight. After the solvent was removed by rotary evaporation, the residue was purified by column chromatography over silica gel using 10:1 CH₂Cl₂/MeOH and then 8:1:0.1 CH₂Cl₂/MeOH/Et₃N as the eluents to give an off-white powder (109 mg, 72%). ¹H NMR (400 MHz, CDCl₃/CD₃OD = 1:1, δ): 3.95 (br, 3H), 3.79 (br, 3H), 3.74 (s, 3H), 3.50 (br, 2H), 3.17 (m, 2H), 2.88 (m, 2H), 2.44 (t, 1H), 2.40–0.77 (a series of m), 0.66 (s, 9H). ¹³C NMR (100 MHz, CDCl₃/CD₃OD = 1:1, δ): 176.0, 175.0, 172.4, 79.9, 73.4, 72.6, 68.4, 63.0, 59.4, 53.2, 51.5, 47.7, 46.9, 46.5, 42.7, 40.2, 36.9, 35.6, 34.0, 32.6, 28.8, 28.3, 27.3, 23.9, 23.0, 17.6, 12.9, 9.3, 7.7. ESI MS (*m/z*): [M + H]⁺ calcd for C₇₉H₁₂₆N₄O₁₁S 1341.9499, found 1341.9411.

Compound 11. Compound 10 was hydrolyzed by standard procedures using 10 equiv of LiOH.²⁸ The hydrolyzed product (50 mg, 0.038 mmol), BOP (84 mg, 0.190 mmol), and HOBt (26 mg, 0.190 mmol) were dissolved in DMF (30 mL), followed by the addition of DIPEA (66 μL, 0.381 mmol). The mixture was allowed to react in a microwave reactor at 100 °C for 1 h, cooled to room temperature, and poured into a dilute HCl solution (0.05 M, 100 mL). The precipitate was collected, dried, and purified by column chromatography over silica gel using 8:1 CH₂Cl₂/CH₃OH as the eluent to give an ivory powder (30 mg, 60%). ¹H NMR (400 MHz, CDCl₃/CD₃OD = 1:1, δ): 4.48 (br, 1H), 3.93 (br, 3H), 3.79 (br, 3H), 3.52 (br, 3H), 3.09 (m, 1H), 2.88 (m, 1H), 2.440 (t, 1H), 2.34–0.74 (a series of m), 0.69 (s, 9H). ¹³C NMR (100 MHz, CDCl₃/CD₃OD = 1:1, δ): 176.1, 74.3, 73.1, 69.4, 48.1, 47.8, 47.5, 43.2, 43.0, 40.9, 37.5, 36.6, 36.2, 35.9, 34.5, 33.7, 33.3, 32.7, 31.0, 29.6, 28.8, 25.5, 28.2, 28.1, 27.9, 24.5, 23.9, 20.6, 18.3, 13.8, 13.6, 9.9. ESI MS (*m/z*): [M + Na]⁺ calcd for C₇₈H₁₂₄N₄O₁₀SNa 1331.8936, found 1331.8909.

Compound 6. Compound 11 (62 mg, 0.047 mmol), methyl 2-azidoterephthalate (13 mg, 0.062 mmol), CuSO₄·5H₂O (24 mg, 0.095 mmol), and sodium ascorbate (38 mg, 0.189 mmol) were dissolved in a 2:1:1 mixture of THF/methanol/water (0.8 mL) and stirred at 40 °C overnight. The reaction mixture was concentrated by rotary evaporation and poured into water (50 mL). The precipitate was collected, dried, and purified by column chromatography

over silica gel, using 12:1 CH₂Cl₂/CH₃OH as the eluent to give an ivory powder (51 mg, 70%). ¹H NMR (400 MHz, CDCl₃/CD₃OD = 1:1, δ): 8.24–8.07 (br, 4 H), 4.53 (br, 1H), 3.97 (s, 3H), 3.93 (br, 3H), 3.79 (br, 3H), 3.73 (s, 3H), 3.43 (br 3H), 2.35–0.78 (a series of m), 0.66 (m, 9H). ¹³C NMR (100 MHz, CDCl₃/CD₃OD = 1:1, δ): 176.6, 175.4, 170.5, 165.7, 136.7, 134.9, 131.9, 128.0, 88.1, 76.8, 73.5, 68.7, 63.2, 53.5, 42.9, 42.8, 42.6, 42.4, 40.2, 40.0, 36.9, 36.5, 36.3, 35.9, 35.5, 35.2, 32.0, 28.1, 27.6, 27.2, 26.3, 23.7, 23.1, 17.7, 12.9. ESI MS (*m/z*): [M + H]⁺ calcd for C₈₈H₁₃₄N₇O₁₄S 1544.9704, found 1544.9699.

Compound 5. Compound 6 (37 mg, 0.024 mmol) was dissolved in MeOH (1 mL), and a solution of 2 M LiOH (0.2 mL, 0.40 mmol) was added. The reaction was stirred at room temperature and monitored by TLC. After the hydrolysis was complete, the organic solvent was removed by rotary evaporation. After the addition of a dilute HCl solution (50 mL, 0.05 M), the precipitate formed was collected by centrifugation, washed with water, and dried in vacuo to give a white powder (22 mg, 61%). ¹H NMR (400 MHz, CDCl₃/CD₃OD = 1:1, δ): 8.24–8.05 (br, 4 H), 4.47 (br, 1H), 3.93 (br, 3H), 3.79 (br, 3H), 3.50 (br, 3H), 2.32–0.77 (a series of m), 0.67 (m, 9H). ¹³C NMR (100 MHz, CDCl₃/CD₃OD = 1:1, δ): 177.3, 176.1, 171.6, 166.7, 166.4, 137.4, 135.6, 132.8, 132.6, 132.2, 128.7, 89.1, 77.4, 74.7, 74.2, 69.5, 54.2, 47.7, 47.6, 47.5, 47.4, 43.4, 43.2, 43.0, 41.0, 40.8, 40.7, 37.5, 37.2, 37.0, 36.2, 36.0, 36.2, 35.9, 34.4, 33.7, 33.3, 32.7, 32.6, 31.1, 29.6, 28.3, 28.0, 27.9, 24.4, 23.9, 23.8, 18.4, 13.7, 13.5. ESI MS (*m/z*): [M + H]⁺ calcd for C₈₆H₁₃₀N₇O₁₄S 1516.9391, found 1516.9350.

Compound 12. The same procedure as in the synthesis of compound 5 was followed to give 12 as an off-white powder (66%). ¹H NMR (400 MHz, CDCl₃/CD₃OD = 1:1, δ): 8.22–8.07 (br, 4 H), 4.45 (br, 1H), 3.95 (br, 3H), 3.79 (br, 3H), 3.49 (br, 3H), 2.31–0.76 (a series of m), 0.68 (m, 9H). ¹³C NMR (100 MHz, CDCl₃/CD₃OD = 1:1, δ): 177.3, 176.1, 171.6, 166.7, 166.4, 137.4, 135.6, 132.8, 132.6, 132.2, 128.7, 89.1, 77.4, 74.7, 74.2, 69.5, 54.2, 47.7, 47.6, 47.5, 47.4, 43.4, 43.2, 43.0, 41.0, 40.8, 40.7, 37.5, 37.2, 37.0, 36.2, 36.0, 36.2, 35.9, 34.4, 33.7, 33.3, 32.7, 32.6, 31.1, 29.6, 28.3, 28.0, 27.9, 24.4, 23.9, 23.8, 18.4, 13.7, 13.5. ESI MS (*m/z*): [M – H]⁺ calcd for C₈₆H₁₂₈N₇O₁₄S 1514.9245, found 1514.9229.

ASSOCIATED CONTENT

Supporting Information

General experimental methods and the NMR data for the key compounds. This material is available free of charge via the Internet at <http://pubs.acs.org>.

AUTHOR INFORMATION

Corresponding Author

*Phone: 515-294-5845. Fax: 515-294-0105. E-mail: zhaoy@iastate.edu.

Notes

The authors declare no competing financial interest.

ACKNOWLEDGMENTS

We thank NSF (DMR-1005515) for supporting the research.

REFERENCES

- (1) Yeagle, P. *The Structure of Biological Membranes*, 2nd ed.; CRC Press: Boca Raton, 2005.
- (2) (a) Hopkins, A. L.; Groom, C. R. *Nat. Rev. Drug Discovery* **2002**, *1*, 727. (b) Lundstrom, K. *Curr. Protein Pept. Sci.* **2006**, *7*, 465.
- (3) (a) Zhao, Y.; Zhong, Z.; Ryu, E.-H. *J. Am. Chem. Soc.* **2007**, *129*, 218. (b) Cho, H.; Zhong, Z.; Zhao, Y. *Tetrahedron* **2009**, *65*, 7311.
- (4) (a) Zhang, S.; Zhao, Y. *Chem.—Eur. J.* **2011**, *17*, 12444. (b) Cho, H.; Zhao, Y. *J. Am. Chem. Soc.* **2010**, *132*, 9890.
- (5) Cho, H.; Widanapathirana, L.; Zhao, Y. *J. Am. Chem. Soc.* **2011**, *133*, 141.
- (6) Widanapathirana, L.; Zhao, Y. *Langmuir* **2012**, *28*, 8165.

- (7) Wang, T.; Widanapathirana, L.; Zhao, Y.; Hong, M. *Langmuir* **2012**, *28*, 17071.
- (8) (a) Granja, J. R.; Ghadiri, M. R. *J. Am. Chem. Soc.* **1994**, *116*, 10785. (b) Sakai, N.; Mareda, J.; Matile, S. *Acc. Chem. Res.* **2005**, *38*, 79. (c) Das, G.; Talukdar, P.; Matile, S. *Science* **2002**, *298*, 1600. (d) Sakai, N.; Sorde, N.; Matile, S. *J. Am. Chem. Soc.* **2003**, *125*, 7776. (e) Ma, L.; Melegari, M.; Colombini, M.; Davis, J. T. *J. Am. Chem. Soc.* **2008**, *130*, 2938. (f) Chen, L.; Si, W.; Zhang, L.; Tang, G.; Li, Z.-T.; Hou, J.-L. *J. Am. Chem. Soc.* **2013**, *135*, 2152.
- (9) (a) Bailey, M.; Brown, C. J. *Acta Crystallogr.* **1967**, *22*, 387. (b) Sledz, M.; Janczak, J.; Kubiak, R. *J. Mol. Struct.* **2001**, *595*, 77.
- (10) Widanapathirana, L.; Li, X.; Zhao, Y. *Org. Biomol. Chem.* **2012**, *10*, 5077.
- (11) Kinsky, S. C.; Haxby, J. A.; Zopf, D. A.; Alving, C. R.; Kinsky, C. B. *Biochemistry* **1969**, *8*, 4149.
- (12) Stein, W. D. *Carriers and Pumps: An Introduction to Membrane Transport*; Academic Press: San Diego, 1990.
- (13) Nezil, F. A.; Bloom, M. *Biophys. J.* **1992**, *61*, 1176.
- (14) Holthuis, J. C. M.; van Meer, G.; Huitema, K. *Mol. Membr. Biol.* **2003**, *20*, 231.
- (15) (a) Demel, R. A.; Bruckdor, K. R.; van Deene, L. L. *Biochim. Biophys. Acta* **1972**, *255*, 321. (b) Papahadjopoulos, D.; Nir, S.; Ohki, S. *Biochim. Biophys. Acta* **1972**, *266*, 561.
- (16) New, R. R. C. *Liposomes: A Practical Approach*; IRL Press: Oxford, 1990.
- (17) Cho, H.; Zhao, Y. *Langmuir* **2011**, *27*, 4936.
- (18) Davis, J. T.; Okunola, O.; Quesada, R. *Chem. Soc. Rev.* **2010**, *39*, 3843.
- (19) Struck, D. K.; Hoekstra, D.; Pagano, R. E. *Biochemistry* **1981**, *20*, 4093.
- (20) Another reason was the flexibility in the macrocycle introduced by the inserted L-cysteine. Our earlier work indicates that rigidity in the macrocycle facilitates the pore formation: Widanapathirana, L.; Zhao, Y. *J. Org. Chem.* **2012**, *77*, 4679.
- (21) (a) Yang, J.; Marendaz, J. L.; Geib, S. J.; Hamilton, A. D. *Tetrahedron Lett.* **1994**, *35*, 3665. (b) Zimmerman, S. C.; Zeng, F. W.; Reichert, D. E. C.; Kolotuchin, S. V. *Science* **1996**, *271*, 1095.
- (22) James A, H. In *Carbon-13 NMR Spectroscopy of Biological Systems*; Academic Press: San Diego, 1995; p 117.
- (23) (a) Kamp, F.; Hamilton, J. A. *Proc. Natl. Acad. Sci. U.S.A.* **1992**, *89*, 11367. (b) Kamp, F.; Zakim, D.; Zhang, F.; Noy, N.; Hamilton, J. A. *Biochemistry* **1995**, *34*, 11928. (c) Hamilton, J. A.; Guo, W.; Kamp, F. *Mol. Cell. Biochem.* **2002**, *239*, 17.
- (24) Cubberley, M. S.; Iverson, B. L. *J. Am. Chem. Soc.* **2001**, *123*, 7560.
- (25) Widanapathirana, L.; Zhao, Y. *J. Org. Chem.* **2012**, *77*, 4679.
- (26) In CCl₄ and heptane, the dimerization constant of carboxylic acids is 10³–10⁴ M⁻¹, equivalent to 4–5 kcal/mol in binding free energy. See: Wenograd, J.; Spurr, R. A. *J. Am. Chem. Soc.* **1957**, *79*, 5844. Goodman, D. S. *J. Am. Chem. Soc.* **1958**, *80*, 3887. Since the hydrophobic core of the membrane essentially comprises hydrocarbon, a similar binding free energy is expected.
- (27) Boccalon, M.; Iengo, E.; Tecilla, P. *J. Am. Chem. Soc.* **2012**, *134*, 20310.
- (28) Zhao, Y.; Zhong, Z. *J. Am. Chem. Soc.* **2005**, *127*, 17894.
- (29) Struthers, H.; Spingler, B.; Mindt, T. L.; Schibli, R. *Chem.—Eur. J.* **2008**, *14*, 6173.
- (30) (a) Morris, W.; Taylor, R. E.; Dybowski, C.; Yaghi, O. M.; Garcia-Garibay, M. A. *J. Mol. Struct.* **2011**, *1004*, 94. (b) Pokhodylo, N. T.; Matychuk, V. S. *J. Heterocycl. Chem.* **2010**, *47*, 415.